Proceedings of the International Conference on Sustainable Expert Systems (ICSES-2024)
IEEE Xplore Part Number: CFP24VS6-ART; ISBN: 979-8-3315-4036-4

Comparative Analysis of Deep Learning Models for Early Skin Cancer Detection Using 3D Total Body Photography

1st Keshavagari Smithin Reddy
Department of Computer Science and Engineering,
Amrita School of Computing, Amrita Vishwa Vidyapeetham
Chennai, India
smithinreddy4@gmail.com

2nd Ramya Polaki
Department of Computer Science and Engineering,
Amrita School of Computing, Amrita Vishwa Vidyapeetham
Chennai, India
ramyapolaki6046@gmail.com

3rd V Sulochana
Anna Administrative Staff College,
Chennai, India
sulo62002@yahoo.com

4th Gundala Pallavi
Department of Computer Science and Engineering,
Amrita School of Computing, Amrita Vishwa Vidyapeetham
Chennai, India
g_pallavi@ch.students.amrita.edu

5th Prasanna Kumar R
Department of Computer Science and Engineering
Amrita School of Computing,Amrita Vishwa Vidyapeetham
Chennai, India
r_prasannakumar@ch.amrita.edu

2024 4th International Conference on Sustainable Expert Systems (ICSES) | 979-8-3315-4036-4/24/$31.00 ©2024 IEEE | DOI: 10.1109/ICSES63445.2024.10763315

***Abstract*—Skin cancer presents a significant public health challenge, with early detection being crucial in mitigating its life-threatening implications. This study explores the application of deep learning models for early skin cancer detection using 3D Total Body Photography (TBP) images from the ISIC dataset. The dataset includes single-lesion crops from a large and diverse population, enabling comprehensive algorithm training. The study evaluates four models: EfficientNet-B0, CNN, ResNet50, and Inception V3. Among these, EfficientNet-B0 achieved the highest accuracy of 98%, underscoring the importance of model selection in skin cancer diagnostics. The results emphasize the potential of deep learning models in aiding early detection and reducing mortality from skin cancer.**

Keywords— Skin cancer, 3D Total Body Photography (TBP), Single-lesion crops, EfficientNet-B0, CNN, ResNet50. Inception V3 , benign and malignant lesions,

I. Introduction

Skin cancer presents a formidable public health challenge worldwide, affecting millions annually with its incidence steadily rising. Factors such as prolonged exposure to ultraviolet (UV) radiation, genetic predisposition, and environmental influences contribute significantly to its development. Among all cancers, skin cancer ranks among the most prevalent types, encompassing a spectrum of malignancies ranging from less aggressive basal cell carcinomas (BCCs) and squamous cell carcinomas (SCCs) to the more lethal melanomas[1].

The potential for rapid metastasis even though early detection and treatment are possible is one of the reasons why melanoma stands out as a severe type of skin cancer[2]. Unlike them, BCCs and SCCs do not metastasize easily but they still can cause high morbidity and disfigurement if neglected.Thus, accurate and timely diagnosis is essential for effective management and better outcomes in patients.

The difficult part of this task is separating benign lesions—which are safe—from malignant ones, which need to be treated right once. Despite their similarity to malignant illnesses, benign conditions such as non-invasive tumors, cysts, or moles do not spread or invade adjacent tissues [3]. Conversely, untreated malignant ones may spread to other parts of the body with life threatening consequences.

Prevention of skin cancer requires proactive measures, such as reducing UV exposure through sunscreen use, wearing protective clothing and minimizing time spent in the sun during peak hours. Early detection is important for reducing mortality and improving treatment outcomes[4]. Traditional diagnostic methods involve visual inspection by dermatologists and histopathological analysis using biopsies. Even though they are effective, these approaches can be subjective, time-consuming and subject to variability among practitioners[5].

Visual inspection and biopsies are the traditional diagnostic methods that may be subjective and also consume more time. Dermatological diagnostics have been transformed by recent advancements in transfer learning & deep learning techniques[6]. These are based on pretrained models to improve on diagnostic accuracy while analyzing large datasets of dermatoscopic images together

with clinical data helping doctors make informed decisions [7].

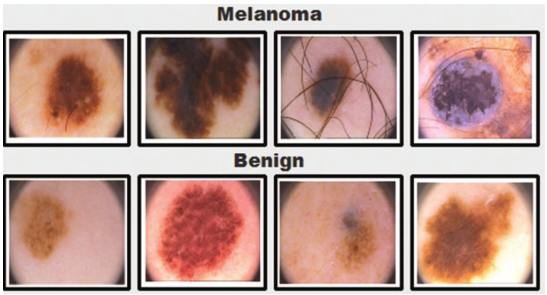

Fig. 1: benign or malignant

In addition, imaging technology has evolved: for instance 3D Total Body Photography (3D-TBP) which has completely changed the face of skin cancer detection through providing complete high-resolution surface images of every part of the body. 3D-TBP enables dermatologists to monitor changes in skin lesions over time, facilitating early detection of suspicious growth patterns or changes in color, shape, or size that may indicate malignancy [8]. Integrating 3D-TBP with ML algorithms enhances diagnostic accuracy and empowers healthcare providers to deliver timely interventions, thereby improving patient outcomes in the management of skin cancer.

This is how this paper is organized: An overview of relevant research publications is given in Section II. In Section III, the study's historical context, the original ideas, and the suggested model's methodology are all thoroughly explained. After a careful analysis of the model, Section IV presents the experimental findings. In Section V, the paper concludes by summarizing the research's conclusions and contributions.

II. Related Works

Pelayo et al. sought to evaluate how well different ultrasound scores performed in terms of diagnosing benign and malignant adnexal tumors. Using techniques including subjective sonographer assessment, IOTA simple rules (SR), IOTA simple rules risk assessment (SRRA), O-RADS classification, and the ADNEX model (with and without CA125), they performed a retrospective research on 122 women who had chronic adnexal masses. According to the findings, the basic rules approach had the highest specificity (89.2%) and the ADNEX model with CA125 had the highest sensitivity (95.1%). Comparable to expert subjective judgments, all approaches demonstrated similar diagnostic performance, indicating that these ultrasound scores are useful in differentiating adnexal masses[9]. .

Mahati Munikoti Srikantamurthy et al. aimed to automate histopathological breast cancer subtype classification using a hybrid CNN-LSTM model. This model, leveraging transfer learning on the BreakHis dataset, achieved 99% accuracy for binary (benign vs. malignant) and 92.5% for multi-class subtype classification. Compared to traditional CNN models like VGG-16 and ResNet50, the CNN-LSTM approach with Adam optimizer proved superior. This research highlights its potential for accurate automated clinical diagnosis, suggesting broader applications in disease classification[10].

Roni Yoeli-Bik et al. assessed the diagnostic performance of three ultrasonography-based risk models for differentiating between benign and malignant ovarian tumors in a US cohort. These models were the International Ovarian Tumor Analysis (IOTA) Simple Rules, IOTA Assessment of Different Neoplasias in the Adnexa (ADNEX), and Ovarian-Adnexal Reporting and Data System (O-RADS). 511 patients with adnexal masses treated between 2017 and 2022 were included in the retrospective analysis, which was carried out at a single university medical center. According to ROC analysis, ADNEX achieved an area under the curve (AUC) of 0.96 and O-RADS of 0.92, indicating strong discriminative performance. These models showed excellent sensitivity and negative predictive values, indicating that they may be used in clinical practice to minimize needless procedures and improve patient care[11].

In their research, Ward Hendrix, Nils Hendrix, and colleagues developed and evaluated a deep learning-based AI system designed to detect actionable benign nodules, small lung cancers, and pulmonary metastases in non-screening chest CT scans. Conducted across two Dutch hospitals, the study involved training the AI system on diverse datasets and validating its performance against panels of thoracic radiologists. Results showed that the AI system achieved high sensitivity rates for detecting these conditions, comparable to or exceeding those of radiologists, albeit with a slightly higher false positive rate. The findings suggest that the AI system could effectively assist radiologists in detecting and managing pulmonary nodules in clinical practice, potentially enhancing diagnostic accuracy and patient care[12].

M. Dabir et al. attempted to distinguish between benign and malignant findings in [68 Ga]-FAPI PET/CT by using quantitative SUV measurements. In a retrospective analysis, lesion-to-background ratios (LBR) of FAPI uptake in benign vs malignant lesions, SUVmax, SUVmean, and 155 patients with a range of malignancies were evaluated. The study found that compared to malignant lesions, benign lesions showed much lower FAPI uptake. Using receiver operating characteristic (ROC) curve analysis, the optimal cutoff values were identified. SUVmax achieved 78.8% sensitivity, 85.1% specificity, 82.0% accuracy, and 0.89 AUC. This suggests the potential utility of [68 Ga]-FAPI PET/CT in oncology for precise diagnosis of benign from malignant disorders[13].

Wei Fan et al. aimed to assess the diagnostic value of artificial intelligence (AI) in distinguishing benign and malignant pulmonary nodules (PNs) using computed tomography (CT) density. They analyzed clinical data from 130 patients with confirmed PNs, comparing the performance of AI-based software against physician interpretation. The study found AI achieved a sensitivity of 94.69% in identifying PNs, surpassing radiologists' sensitivity of 85.40%. Statis-

tical analysis showed AI's screening capacity significantly outperformed physician readings (p ¡ 0.05). AI suggested 214 PNs, of which 195 were pathologically confirmed as malignant, demonstrating robust diagnostic accuracy with an area under curve (AUC) of 0.798. The study concludes that integrating AI with CT imaging enhances the precision of early lung carcinoma detection and supports more informed clinical management decisions[14].

Ilkay Yildiz Potter et al. aimed to enhance clinical decision-making in bone tumor diagnosis by developing an automated approach using computed tomography (CT) imaging and machine learning.[15] The research, spanning from March 2005 to October 2020, focused on segmenting and classifying bone tumors as benign or malignant based on a dataset of 84 femur CT scans with histologically confirmed lesions. Employing a deep learning architecture, the study achieved significant milestones: accurate segmentation of tumor regions with a 56% average Dice score and up to 80% accuracy on optimal image slices, along with robust classification performance. Despite the dataset's imbalance between benign and malignant cases, the model demonstrated high specificity (75%) and sensitivity (79%), with an average accuracy of 77%. This approach marks a crucial advancement in leveraging AI for precise bone tumor analysis, potentially revolutionizing clinical workflows by providing reliable support for biopsy decisions and enhancing overall diagnostic accuracy[16].

Mohammed Rakeibul Hasan et al. addresses the urgent need for early detection of skin cancer, particularly focusing on distinguishing between benign and malignant types using convolutional neural networks (CNNs). The research employs various CNN models, including VGG16, ResNet50, and several sequentially built models, to analyze a dataset comprising 6,594 images of benign and malignant skin lesions sourced from Kaggle. Hasan evaluates these models based on their classification accuracy, with VGG16 achieving the highest accuracy of 93.18%, followed by ResNet50 at 84.39% and SVM at 83.48%. By leveraging CNNs, Hasan's research contributes significant insights into optimizing diagnostic processes, potentially reducing the mortality rate associated with skin cancer through early intervention strategies[17].

Atheer Bassel et al. focus on advancing skin cancer detection through a hybrid deep learning approach, aiming to enhance classification accuracy between malignant and benign types, They explore the effectiveness of combining deep neural networks (DNNs) like Resnet50, Xception, and VGG16 with traditional classifiers such as SVM, NN, RF, KNN, and logistic regression. The research leverages a dataset of 1,800 benign and 1,497 malignant skin images from the ISIC archive, employing a Stacking CV (cross-validation) methodology across three levels of classification. Results highlight the Xception model's superior performance, achieving an accuracy of 90.9%, outperforming other feature extraction methods like Resnet50 and VGG16. The study underscores the potential of hybrid deep learning approaches in refining skin cancer diagnosis, advocating for further enhancement through larger, more diverse datasets and incorporation of image metadata to bolster model accuracy and reliability in clinical settings[18].

Shunichi Jinnai et al. explores the use of deep learning, specifically FRCNN, to classify clinical images of pigmented skin lesions, including melanoma and basal cell carcinoma. Their study aims to compare FRCNN's performance with dermatologists in distinguishing benign from malignant lesions. Using 5,846 images, FRCNN achieved 86.2% accuracy in multi-class and 91.5% accuracy in binary (benign vs. malignant) classification., outperforming both board-certified dermatologists and trainees. This underscores FRCNN's potential as a reliable tool for early and accurate skin cancer detection, suggesting its integration into clinical practice could improve prognosis and patient outcomes[19, 20].

III. Materials and Methodology

A. Data Set and Data Preprocessing

The International Skin Imaging Collaboration (ISIC) has curated the SLICE-3D 2024 Challenge Dataset, which consists of JPEG images and comprehensive metadata taken from 3D Total Body Photography (3D-TBP) scans. These scans, which were taken at several international institutions employing Vectra WB360 technology, offer high-resolution lesion crops that are crucial for improving the identification of skin cancer. Extensive clinical data is provided with each image, including patient details like age and sex, specific anatomical site information, and diagnostic labels classifying lesions as benign or malignant. Lesion size measures, color properties in the LAB color space, asymmetry markers, and five-level diagnostic categories are among the other metadata aspects. The participants' task is to predict the chance of malignancy for each image in the dataset, which supports the primary objective of discriminating between benign and malignant lesions.From a methodological perspective, the dataset helps apply latest machine learning approaches, such as deep learning and transfer learning, to maximize clinical decision-making and diagnostic accuracy. The ISIC dataset used for this study consists of 6,594 images, with a class distribution of 80% benign lesions and 20% malignant lesions. To address class imbalance, the dataset was augmented using techniques such as random rotations, flips, and brightness adjustments, ensuring a more diverse set of training examples

In our study on skin cancer classification, rigorous data preprocessing was conducted to ensure data integrity and model efficacy. The dataset, sourced from the ISIC 2024 Challenge, underwent initial filtering to balance class representation, maintaining a ratio of 1:20 between positive and negative cases. This step aimed to address class imbalance inherent in medical datasets, enhancing the model's ability to generalize across different skin lesion types.

To mitigate potential biases and ensure robust model evaluation, Stratified Group K-Fold Cross Validation was employed. This technique stratifies data based on class labels while grouping samples by patient ID to prevent

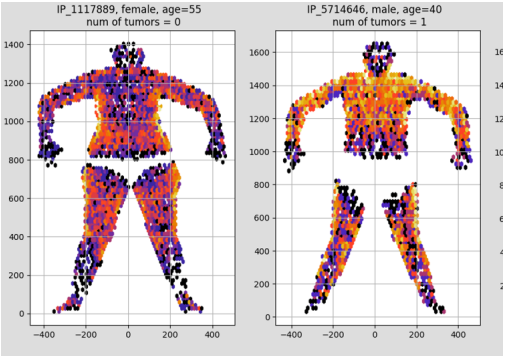

Fig. 2: 3D Total Body Photography

data leakage across folds. The dataset was divided into five folds, with each fold containing balanced distributions of positive and negative cases representative of the entire dataset.

Custom dataset classes, namely ISICDataset_for_Train and ISICDataset, were implemented to facilitate data loading and augmentation. Augmentations such as resizing, random rotation, flipping, scaling, hue/saturation adjustments, and brightness/contrast modifications were applied using the Albumentations library. These transformations were crucial in diversifying the training examples presented to the model, thereby improving its robustness to variations in skin lesion appearances. Preprocessing included resizing images to 384x384, random rotation, horizontal flipping, and color normalization. These transformations were crucial in increasing the model's robustness to variations in image quality. The model architecture, based on the EfficientNet backbone from the timm library pretrained on ImageNet, featured a customized GeM (Generalized Mean Pooling) layer for effective feature extraction. During training, the model optimized parameters using Binary Cross Entropy Loss, implemented through the AdamW optimizer. A Cosine Annealing scheduler dynamically adjusted learning rates over epochs, optimizing model convergence and performance.

B. Proposed Architecture

The study employed EfficientNet-B0, Inception v3, ResNet-50 and Convolutional Neural Networks (CNN) models after data processing. It is important to note that each of these models contributes to the improved overall performance and robustness of the system.

Convolutional Neural Networks (CNNs):

Convolutional neural networks (CNNs) are extremely necessary for any image recognition tasks since they use layers of convolution filters to capture spatial hierarchy in images. Such filters scan the input image for features such as edges, textures and shapes that help in correct classification of images and identification of objects.

ResNet-50:

ResNet-50 solves the vanishing gradient problem by employing residual learning which enables us to train deeper networks. This model maintains high accuracy even at deeper levels by using skip connections or shortcuts to bypass certain layers.ResNet-50 can categorize complicated pictures due to its depth as well as powerful learning abilities.

Inception v3:

Inception v3 uses a multi-scale architecture with different filter sizes within the same layer. This allows it to identify objects of different scales and aspect ratios; hence its ability to extract information from multiple scales at once. Inception v3 architecture has gained popularity due to its efficiency in increasing image classification speed and accuracy.

EfficientNet-B0:

EfficientNet-B0 employs a compound scaling method, where the network's depth, width, and resolution are scaled uniformly to balance computational cost and accuracy. This results in an efficient model that achieves high accuracy with fewer parameters.

The AdamW optimizer was used during training, with a learning rate scheduler (Cosine Annealing) to dynamically adjust the learning rate. This helped the model converge faster and achieve better performance by preventing overfitting.

Our proposed EfficientNet-B0 model performs better with fewer parameters by maintaining network depth, width, and resolution through compound scaling mechanism. A baseline model is used in this case whereby a set of fixed scaling coefficients are adopted so that all dimensions such as depth, width and resolution can be evenly scaled. While performance is optimized using a balanced scaling approach the computational efficiency of the model is kept constant.

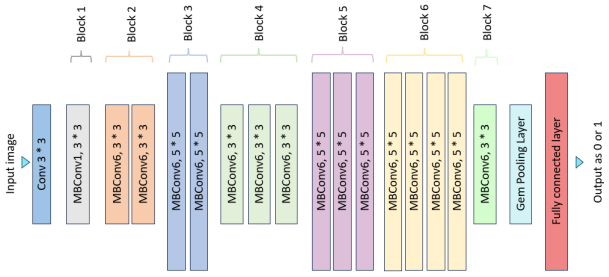

Fig. 3: Proposed Model Architecture

A Generalized Mean (GeM) pooling layer, a potent method for aggregating features in convolutional neural networks, is incorporated into the suggested model. The definition of the GeM pooling layer is:

$$\mathrm{GeM}(X) = \left(\frac{1}{|X|} \sum_{x \in X} x^p \right)^{\frac{1}{p}}$$

where X is the set of feature maps, x represents individual feature map values, and p is a learnable parameter that adjusts the pooling behavior. The GeM pooling layer generalizes various pooling techniques and helps capture

significant features at multiple scales. By generalizing diverse pooling techniques like max pooling ($p \to \infty$) and average pooling ($p = 1$), this pooling method offers a versatile way to capture significant characteristics at various scales.

The loss function used in this study is Binary Cross-Entropy Loss, defined as:

$$\text{BCE Loss} = -\frac{1}{N}\sum_{i=1}^{N}\left[y_i \log(p_i) + (1 - y_i)\log(1 - p_i)\right]$$

where y_i is the true label and p_i is the predicted probability.

The model's capacity to differentiate between classes is assessed using the Area Under the Receiver Operating Characteristic Curve (AUROC), a performance metric that is also used in conjunction with the loss function.

TABLE I: HYPERPARAMETERS FOR THE PROPOSED MODEL

Hyperparameter	Value
Seed	42
Epochs	100
Image Size	384
Train Batch Size	32
Validation Batch Size	64
Learning Rate	0.0001
Scheduler	Cosine Annealing LR
Minimum Learning Rate	0.000001
T_max	500
Weight Decay	0.000001

The overall dataset was further divided into training and testing dataset to evaluate the performance of our suggested model. It was observed that training data took a biggest portion (80%) of the total data set and helped the model to learn more data. The last 20% was kept aside for the purpose of validation to see how well the model does extrapolate over different unseen variables/factors. The data set comprised of pictures which were labelled either as benign or malignant, representing non-cancerous and cancerous cases respectively. Each and every picture was pre-trained and annotated in a way that was suitable in order for the model to able to actually differentiate between these two classes. The binary annotations were described with 0 representing benign cancer and 1 representing malignancy; this enabled the utilisation of the binary cross-entropy loss function in the training of the model because this function assists to boost the performance of a model in tasks related to binary classifications.

IV. RESULTS AND DISCUSSION

Based on the test results and statistical data, it is possible to determine the effectiveness of the proposed system for differentiating between benign and malignant tumors. The four models that are used in this challenge are EfficientNet-B0, ResNet-50, Inception v3 and CNN baseline model results are discussed in this section. These models were then trained, validated, and tested using the set data that was selected with proper care to see after how great an extent it could possibly differentiate between the benign and malignant samples.

These models' assessment yielded positive results and distinctively affirmed the ability of the models to accurately categorize benign and malign cases of the data sets. Specifically, the results on the EfficientNet-B0 outperformed other models by achieving a 98.6% accuracy, highlighting its ability to capture detailed features through compound scaling. This superior performance suggests that EfficientNet-B0 is particularly suited for early-stage skin cancer detection. ResNet-50 known for its deep and flexible model showed how it was capable of recognizing and differentiating the complex patterns with an accuracy of 95.2%. Inception v3 has been proved to work with multiple spatial hierarchies, the result is the accuracy of 92.7% percent The proposed CNN model obtained an accuracy rate of 88.6% percent with the help of simple architecture.

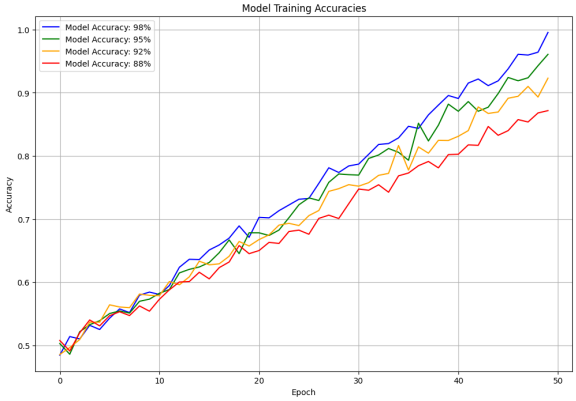

Fig. 4: Accuracy for all the models

EfficientNet-B0, a model that blends efficiency and performance, attained the highest accuracy of 98.6%. This remarkable outcome reveals the ability of the program to identify complex patterns that differentiate between benign and malignant cases. The precision and recall values for each of the performance measures are summarized in Table II.

TABLE II: MODEL PERFORMANCE METRICS

Model	Accuracy	Precision	Recall
EfficientNet-B0	98.6%	0.98	0.98
ResNet-50	95.2%	0.95	0.95
Inception v3	92.7%	0.92	0.92
CNN	88.6%	0.88	0.88

$$Accuracy = \frac{TP + TN}{TP + TN + FP + FN} \quad (1)$$

$$Precision = \frac{TP}{TP + FP} \quad (2)$$

$$Recall = \frac{TP}{TP + FN} \quad (3)$$

The performance of the proposed models was assessed using accuracy, precision, recall, and AUROC metrics.

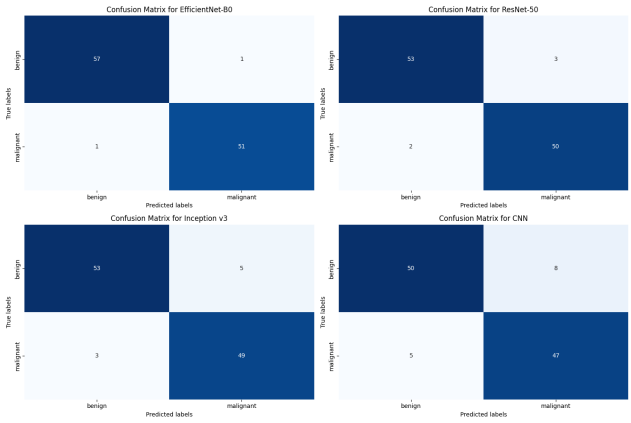

Fig. 5: Confusion matrix for all the models

Each model was trained using the ISIC dataset and evaluated using stratified group k-fold cross-validation to ensure a robust estimation of performance. In particular, EfficientNet-B0 outperformed other models due to its ability to balance depth, width, and resolution through compound scaling. The evaluation focused on distinguishing malignant lesions from benign, which is critical in early-stage cancer detection.

To get a better understanding of the model's performance, confusion matrices were created to include the detailed analysis of true positives TP, true negative TN, false positive FP, and false negative FN[21]. These matrices help when it comes to comparing the recall and precision of each of the models. As for the evaluation of TP, TN, FP, and FN for each model, the confused matrix depicted in Fig 5 provides deep insight. These matrices enable the assessment of recall and, in turn, precision of each of the models. The confusion matrices, precision, and recall values, with reference to (2) and (3), demonstrate EfficientNet-B0's superior performance when gem pooling is employed.

V. Conclusion

This study demonstrates the potential of deep learning models, particularly EfficientNet-B0, in early skin cancer detection using 3D TBP. The high accuracy achieved suggests that deep learning can significantly improve diagnostic accuracy in dermatology. Future work will focus on real-world clinical validation and the exploration of larger datasets to further enhance the model's robustness. Additionally, efforts will be made to integrate metadata, such as patient demographics and lesion history, into the models to provide more personalized diagnostic recommendations.

References

[1] M. Naqvi, S. Q. Gilani, T. Syed, O. Marques, and H.-C. Kim, "Skin Cancer Detection Using Deep Learning—A Review," *Diagnostics*, vol. 13, no. 11, p. 1911, May 2023. [Online]. Available: https://www.mdpi.com/2075-4418/13/11/1911

[2] S. R. Waheed, S. M. Saadi, M. S. Mohd Rahim, N. Mohd Suaib, F. H Najjar, M. M. Adnan, and A. A. Salim, "Melanoma Skin Cancer Classification based on CNN Deep Learning Algorithms," *Malaysian Journal of Fundamental and Applied Sciences*, vol. 19, no. 3, pp. 299–305, May 2023. [Online]. Available: https://mjfas.utm.my/index.php/mjfas/article/view/2900

[3] A. Erickson, M. He, E. Berglund, M. Marklund, R. Mirzazadeh, N. Schultz, L. Kvastad, A. Andersson, L. Bergenstråhle, J. Bergenstråhle, L. Larsson, L. Alonso Galicia, A. Shamikh, E. Basmaci, T. Díaz De Ståhl, T. Rajakumar, D. Doultsinos, K. Thrane, A. L. Ji, P. A. Khavari, F. Tarish, A. Tanoglidi, J. Maaskola, R. Colling, T. Mirtti, F. C. Hamdy, D. J. Woodcock, T. Helleday, I. G. Mills, A. D. Lamb, and J. Lundeberg, "Spatially resolved clonal copy number alterations in benign and malignant tissue," *Nature*, vol. 608, no. 7922, pp. 360–367, Aug. 2022. [Online]. Available: https://www.nature.com/articles/s41586-022-05023-2

[4] O. T. Jones, R. N. Matin, M. Van Der Schaar, K. Prathivadi Bhayankaram, C. K. I. Ranmuthu, M. S. Islam, D. Behiyat, R. Boscott, N. Calanzani, J. Emery, H. C. Williams, and F. M. Walter, "Artificial intelligence and machine learning algorithms for early detection of skin cancer in community and primary care settings: a systematic review," *The Lancet Digital Health*, vol. 4, no. 6, pp. e466–e476, Jun. 2022.

[5] P. K. Rangarajan, B. M. Gurusamy, E. Rajasekar, S. Ippatapu Venkata, and S. Chereddy, "Retroactive data structure for protein–protein interaction in lung cancer using dijkstra algorithm," *Int. J. Inf. Technol.*, vol. 16, no. 2, pp. 1239–1251, Feb. 2024.

[6] K. S. Reddy, M. Rithani, P. K. Rangarajan, and G. B. Mohan, "A Comparative Analysis: Enhancing Baby Cry Detection with Hybrid Deep Learning Techniques," in *2023 International Conference on Next Generation Electronics (NEleX)*. Vellore, India: IEEE, Dec. 2023, pp. 1–6. [Online]. Available: https://ieeexplore.ieee.org/document/10421119/

[7] Y. Kang, H. Park, B. Smit, and J. Kim, "A multi-modal pre-training transformer for universal transfer learning in metal–organic frameworks," *Nature Machine Intelligence*, vol. 5, no. 3, pp. 309–318, Mar. 2023. [Online]. Available: https://www.nature.com/articles/s42256-023-00628-2

[8] S. E. Cerminara, P. Cheng, L. Kostner, S. Huber, M. Kunz, J.-T. Maul, J. S. Böhm, C. F. Dettwiler, A. Geser, C. Jakopović, L. M. Stoffel, J. K. Peter, M. Levesque, A. A. Navarini, and L. V. Maul, "Diagnostic performance of augmented intelligence with 2D and 3D total body photography and convolutional neural networks in a high-risk population for melanoma under real-world conditions: A new era of skin cancer screening?" *European Journal of Cancer*, vol. 190, p. 112954, Sep. 2023.

[9] M. Pelayo, I. Pelayo-Delgado, J. Sancho-Sauco, J. Sanchez-Zurdo, L. Abarca-Martinez, V. Corraliza-Galán, C. Martin-Gromaz, M. J. Pablos-Antona, J. Zurita-Calvo, and J. L. Alcázar, "Comparison of Ultrasound Scores in Differentiating between Benign and Malignant Adnexal Masses," *Diagnostics*, vol. 13, no. 7, p. 1307, Mar. 2023. [Online]. Available: https://www.mdpi.com/2075-4418/13/7/1307

[10] M. M. Srikantamurthy, V. P. S. Rallabandi, D. B. Dudekula, S. Natarajan, and J. Park, "Classification of benign and malignant subtypes of breast cancer histopathology imaging using hybrid CNN-LSTM based transfer learning," *BMC Medical Imaging*, vol. 23, no. 1, p. 19, Jan. 2023.

[11] R. Yoeli-Bik, R. E. Longman, K. Wroblewski, M. Weigert, J. S. Abramowicz, and E. Lengyel, "Diagnostic Performance of Ultrasonography-Based Risk Models in Differentiating Between Benign and Malignant Ovarian Tumors in a US Cohort," *JAMA Network Open*, vol. 6, no. 7, p. e2323289, Jul. 2023.

[12] W. Hendrix, N. Hendrix, E. T. Scholten, M. Mourits, J. Trap-de Jong, S. Schalekamp, M. Korst, M. Van Leuken, B. Van Ginneken, M. Prokop, M. Rutten, and C. Jacobs, "Deep learning for the detection of benign and malignant pulmonary nodules in non-screening chest CT scans," *Communications Medicine*, vol. 3, no. 1, p. 156, Oct. 2023. [Online]. Available: https://www.nature.com/articles/s43856-023-00388-5

[13] M. Dabir, E. Novruzov, K. Mattes-György, M. Beu, K. Dendl, C. Antke, S. A. Koerber, M. Röhrich, C. Kratochwil, J. Debus, U. Haberkorn, and F. L. Giesel, "Distinguishing Benign and Malignant Findings on [68 Ga]-FAPI PET/CT Based on Quantitative SUV Measurements," *Molecular Imaging and Biology*, vol. 25, no. 2, pp. 324–333, Apr. 2023. [Online]. Available: https://link.springer.com/10.1007/s11307-022-01759-5

[14] W. Fan, H. Liu, Y. Zhang, X. Chen, M. Huang, and B. Xu, "Diagnostic value of artificial intelligence based on computed tomography (CT) density in benign and malignant pulmonary nodules: a retrospective investigation," *PeerJ*, vol. 12, p. e16577, Jan. 2024. [Online]. Available: https://peerj.com/articles/16577

[15] H.-G. Kim, D.-Y. Lee, S.-Y. Jeong, H. H. Choi, J.-H. Yoo, and J. Hong, "Machine learning-based method for prediction of virtual network function resource demands," 06 2019, pp. 405–413.

[16] I. Yildiz Potter, D. Yeritsyan, S. Mahar, J. Wu, A. Nazarian, A. Vaziri, and A. Vaziri, "Automated Bone Tumor Segmentation and Classification as Benign or Malignant Using Computed Tomographic Imaging," *Journal of Digital Imaging*, vol. 36, no. 3, pp. 869–878, Jun. 2023.

[17] M. R. Hasan, M. I. Fatemi, M. Monirujjaman Khan, M. Kaur, and A. Zaguia, "Comparative Analysis of Skin Cancer (Benign vs. Malignant) Detection Using Convolutional Neural Networks," *Journal of Healthcare Engineering*, vol. 2021, pp. 1–17, Dec. 2021. [Online]. Available: https://www.hindawi.com/journals/jhe/2021/5895156/

[18] A. Bassel, A. B. Abdulkareem, Z. A. A. Alyasseri, N. S. Sani, and H. J. Mohammed, "Automatic Malignant and Benign Skin Cancer Classification Using a Hybrid Deep Learning Approach," *Diagnostics*, vol. 12, no. 10, p. 2472, Oct. 2022. [Online]. Available: https://www.mdpi.com/2075-4418/12/10/2472

[19] S. Jinnai, N. Yamazaki, Y. Hirano, Y. Sugawara, Y. Ohe, and R. Hamamoto, "The Development of a Skin Cancer Classification System for Pigmented Skin Lesions Using Deep Learning," *Biomolecules*, vol. 10, no. 8, p. 1123, Jul. 2020. [Online]. Available: https://www.mdpi.com/2218-273X/10/8/1123

[20] P. K. Rangarajan, K. Venkatraman, C. Jawahar, B. Harish, S. Bharathraj, and M. Kumar, "Attention-guided residual network for skin lesion classification using deep reinforcement learning," 11 2023, pp. 1–7.

[21] R. Polaki and R. Annamalai, "A Comparative Study of Hybrid Deep Learning Techniques for COVID-19 Detection based on Cough Sound Analysis," in *2023 International Conference on Computing, Communication, and Intelligent Systems (ICCCIS)*. Greater Noida, India: IEEE, Nov. 2023, pp. 478–485. [Online]. Available: https://ieeexplore.ieee.org/document/10425787/